Int. J. Heat Mass Transfer. Vol. 7, pp. 699–708. Pergamon Press 1964. Printed in Great Britain

AN EXPERIMENTAL STUDY OF THERMAL DIFFUSION EFFECTS ON A PARTIALLY POROUS MASS TRANSFER-COOLED HEMISPHERE*

A. F. GOLLNICK JR.†

Massachusetts Institute of Technology, Aerophysics Laboratory, Cambridge, Massachusetts

(*Received* 16 *September* 1963 *and in revised form* 27 *January* 1964)

Abstract—A hemispherical model having a porous nose cap of 40° included angle was tested at Mach 8·07. Helium and freon-13 were injected through the cap into the stagnation region, and the variations of adiabatic wall temperature and heat-transfer coefficient with injection rate were measured. Analytical solutions have been obtained for a laminar stagnation point boundary layer and similar free stream conditions. The analysis differs from earlier work in that the effects of thermal diffusion are included. It is predicted that this thermodynamic coupling may lead to stagnation point recovery temperatures considerably different from the zero injection value. This conclusion, and hence the significance of thermodynamic coupling, is supported by the data, which is in reasonable agreement with the theory. Temperature measurements were made on the insulated model surface downstream of the injection region. It is concluded that the temperature levels on the entire hemispherical surface can be greatly reduced by localized injection in the stagnation region. Helium proved to be more effective in this respect than freon-13.

NOMENCLATURE

c_1, mass concentration of coolant $= \rho_1/\rho$;
c_p, specific heat at constant pressure;
D_{12}, coefficient of diffusion for binary mixture;
D_T, coefficient of thermal diffusion;
f_w, non-dimensional injection rate [equation (4)];
h, heat-transfer coefficient;
k, thermal conductivity;
k_T, thermal diffusion ratio $= D_T/D_{12}$;
$\dot{m}$, total coolant flow rate;
p, pressure;
$\dot{q}$, heat flux;
R, gas constant;
Re, Reynolds number $= \left(\frac{\rho u x}{\mu}\right)_e$;
St, Stanton number $= \frac{h}{(\rho u c_p)_e}$;
T, temperature;
t, thickness of porous cap;
u, streamwise velocity component;
v, normal velocity component (perpendicular to stream);
x, streamwise co-ordinate;
y, normal co-ordinate.

Greek symbols

α, viscous resistance coefficient for porous material;
μ, viscosity;
ρ, density;
θ, angular displacement from hemisphere axis.

Superscripts

$\overline{(\ )}$, quantity normalized with respect to stagnation conditions.

Subscripts

$(\ )_c$, initial (reservoir) coolant condition;
$(\ )_e$, property evaluated at outer edge of boundary layer;
$(\ )_h$, heater condition;
$(\ )_0$, stagnation point condition;
$(\ )_w$, wall condition;

* The research reported herein was supported by the Air Force Office of Scientific Research under Contract AF 49(638)-245.

† Research Engineer.

$( )_{aw}$, adiabatic wall condition;
$( )_1$, coolant property.

1. INTRODUCTION

OVER the past several years much effort has been devoted to the study of mass transfer cooling. The result is a considerable body of theory dealing with the mechanism by which injection of a gaseous coolant through a porous wall on which there exists a high energy, laminar boundary layer can bring about large reductions in heat transfer. Earlier analyses [1, 2, 3] have shown that for both the flat plate and axisymmetric stagnation point cases, the injectant acts in two ways: first, by acting as a disposable heat sink, the coolant blocks the penetration of heat into the structure; secondly, by altering the boundary-layer structure, i.e. by reducing the temperature gradient at the wall, the coolant can reduce the heat-transfer coefficient (Stanton number), thus lowering the overall heat flux level. Indeed, helium injection at a moderate rate can lead to an order of magnitude reduction in heat transfer at an axisymmetric stagnation point.

Experimental results for air and helium injection [4, 5] have corroborated the theoretical predictions with regard to Stanton number. However, though the theory assumed that at a stagnation point ($M_e = 0$) the adiabatic wall temperature was unaffected by injection, observed levels with helium injection were considerably above the free stream stagnation temperature. More recent data for a two dimensional stagnation point [6] exhibits the same behaviour. Available turbulent data [7] indicates the phenomenon is not confined to the laminar boundary layer. A subsequently revised analysis [8] attributes this phenomenon to thermodynamic coupling within the boundary layer, and gives adiabatic wall temperatures which are in fair agreement with the helium data.

The existence of coupling between the mass and energy fluxes in a heterogeneous boundary layer, caused by the presence of thermal-diffusion and diffusion-thermo (the so-called Soret and Dufor effects), has been discussed previously [1]. Order of magnitude estimates, together with the inherent increase in computational complexity, has heretofore resulted in this phenomenon being neglected [1, 2, 3]. It is now argued that though the thermal diffusion induced energy (heat) flux may be small when the overall flux level is high, this is not the case for near adiabatic conditions [8]. This can readily be seen if the appropriate heat balance at the wall is written:

$$\dot{q} = -k_w \left(\frac{\partial T}{\partial y}\right)_w + (\rho v)_w \left(RT \frac{k_T}{c_1}\right)_w \qquad (1)$$

The heat flux to the wall is the sum of the usual Fourier conduction contribution and that due to thermal diffusion. The direction of the latter is determined by the sign of the thermal diffusion ratio (k_T). Kinetic theory indicates this is largely (but not entirely) dependent on the injectant-to-air molecular weight ratio, being negative for helium and positive for freon-13. For an adiabatic condition to exist ($\dot{q} = 0$), the two contributions must balance, implying that the temperature gradient must be non-zero, and of opposite sign to k_T. An adiabatic wall temperature (T_{aw}) may be defined in the usual manner:

$$\dot{q} = h\,(T_w - T_{aw}) \qquad (2)$$

For zero injection, $T_{aw} = T_0$ at an axisymmetric stagnation point. For helium injection through an adiabatic wall $(\partial T/\partial y)_w < 0$, thus $T_{aw} > T_0$, in conformity with existing data. For freon-13, the reverse should be true.

Numerical solutions based on the theory of reference 8 have been obtained [9], corresponding to the stagnation point conditions appropriate to the test program described herein. Calculations were carried out for both low and high molecular weight coolants (helium and freon-13, respectively) for $k_T \equiv 0$ and for $k_T \neq 0$. The resulting theoretical values of Stanton number and adiabatic wall temperature form a basis of comparison for the experimental results presented in the following sections of this paper.

In the absence of conduction and radiation losses, the steady state heat flux at the wall is completely absorbed by the injectant, leading to the relation

$$\dot{q} = (\rho v)_w c_{p_1} (T_c - T_w) \qquad (3)$$

under these circumstances, for an adiabatic wall, $T_w = T_{aw} = T_c$ and the coolant absorbs no heat at all.

A second area of interest pertains to the persistence of mass transfer cooling downstream of the actual injection region. In the case of a flat plate, this insulating effect has been demonstrated analytically [10] and experimentally [11] for air and helium injection. Some data is also available for stagnation point injection on a hemisphere [12]. Additional data, in the form of temperature distributions on an insulated hemispherical surface downstream of a porous nose cap, was obtained as part of this investigation.

2. TEST PROGRAM

2.1 *Model*

The wind tunnel model was designed and built at the Aerophysics Laboratory at M.I.T. It consisted of a hemisphere–cylinder 6 in in diameter and 15 in long overall. The bulk of the hemispherical nose was made of "Lava A", a naturally occurring aluminum silicate supplied by the American Lava Company, Chattanooga, Tenn. When fired this material has satisfactory high temperature characteristics, combined with the low thermal conductivity (8·71 Btu in/ft² h degR) necessary to furnish the desired insulated surface downstream of the injection region.

The injection region itself consisted of a centrally located porous cap (Fig. 1) subtending a total angle of 40° at the hemisphere center. The cap was cast from an inconel powder and sintered. The permeability was uniform, and the porosity was approximately 0·5. Thermal conductivity was estimated to be 10 per cent of that for solid inconel, or 10·4 Btu in/ft² h degR. The cap was attached to a plenum which served as a settling chamber for the injectant. The plenum was loosely packed with glass wool to minimize convection. Surface temperature on the model was measured by 22 No. 30 gauge chromel–alumel thermocouples, of which 10 were distributed over the outer surface of the porous cap (Figs. 1 and 2); 10 were mounted externally on the lava along a single meridian line; and one each was attached to the inner surface of the inconel and the lava, respectively. Surface thermocouples on the cap were welded to the upstream edge of a radial, 0·025 in hole, through which the leads passed into the plenum.

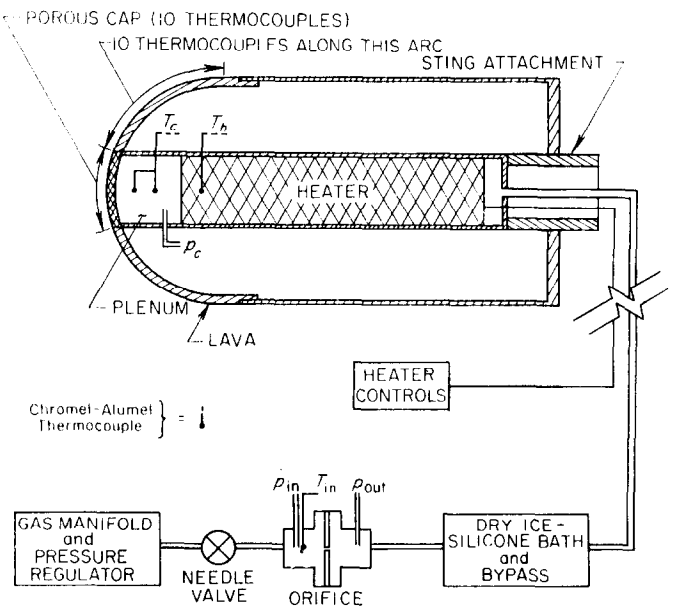

FIG. 1. Model and coolant supply system.

The hole was sealed with a high temperature cement. A similar installation was used on the lava, except the two leads passed from inside the lava into opposite ends of a trough, 0·25 in long, aligned perpendicular to the meridian. The thermocouple was cemented flush with the outer surface, and midway along the trough. This system minimized lead conduction errors by placing the first 0·125 in in an isothermal region. This could not be done on the cap without extensively spoiling the porosity. On the other hand, temperature gradients within the cap were not nearly as severe as for the lava, so such a precaution was unnecessary. The initial or reservoir coolant temperature (T_c) was measured in the plenum by two thermocouples, located on the model axis and distant $\frac{9}{16}$ in and $\frac{15}{16}$ in respectively, from the inner surface of the cap. All thermocouples were rated by the manufacturer as accurate to $\pm\frac{3}{4}$ per cent of the reading in °F, i.e. the uncertainty was always less than ± 8 degF.

The pressure in the plenum (p_c) was measured, and the surface pressure on the model at $\theta = 10°$ recorded via four taps, distributed symmetrically on the cap.

2.2 *Coolants*

The two coolants used during the test were helium and freon-13. The selection of helium for the low molecular weight study was an obvious one. Not only is it the lightest inert gas, but its physical properties are well known over a wide range of temperatures. Coupled with its high heat capacity, these factors make helium a likely coolant for any practical application of mass transfer cooling. To date most of the experimental mass-transfer studies have used helium [4, 5].

The selection of a high molecular weight coolant was not so straightforward. Most gaseous organic compounds are unstable at the desired testing temperatures, the end products being corrosive and toxic. Information about their physical properties is meager, or non-existent. Freon-13, the final choice, is one of the family of fluorinated hydrocarbons [13] produced by E. I. du Pont de Nemours & Co., of Wilmington, Delaware. Its molecular weight (see Table 1) is only moderately high, but it is very stable at elevated temperatures, as well as being non-toxic and non-corrosive. Dr. F. Palmer of du Pont furnished the latest physical data on freon-13, but classic kinetic theory had to be used to predict the variations of viscosity, thermal conductivity and specific heat with temperature.

2.3 *Coolant supply system*

The details of the coolant supply system appear in Fig. 1. Both gases were contained in standard 1·5 ft^3 cylinders, the helium being under 2000 psi and the freon-13 under its saturated vapor pressure (500 psi at 75°F). The gas passed through a pressure regulator which ensured a constant supply pressure of approximately 300 psi. The total coolant flow was metered by a precalibrated sonic orifice. The inlet pressure (p_{in}) was set at predetermined levels by means of the needle valve shown in Fig. 1. Both p_{in} and T_{in} were measured so that the mass flow could be computed. The outlet pressure (p_{out}) was also monitored, to ensure the orifice flow was always sonic.

The model mount was only partly cooled resulting in some preheating of the coolant before it reached the model. This reduced the potential range of wall temperatures available. To minimize this effect a coil immersed in a dry

Table 1. *Some properties of injectants compared with air*

Property	Helium	Air	Freon-13
Molecular weight	4·0	29·0	104·5
Boiling point (°F at 1 atm)	−452·0	< −297·0	−114·6
Specific heat at const. pressure Btu/lb degF)	1·246	0·241	0·207

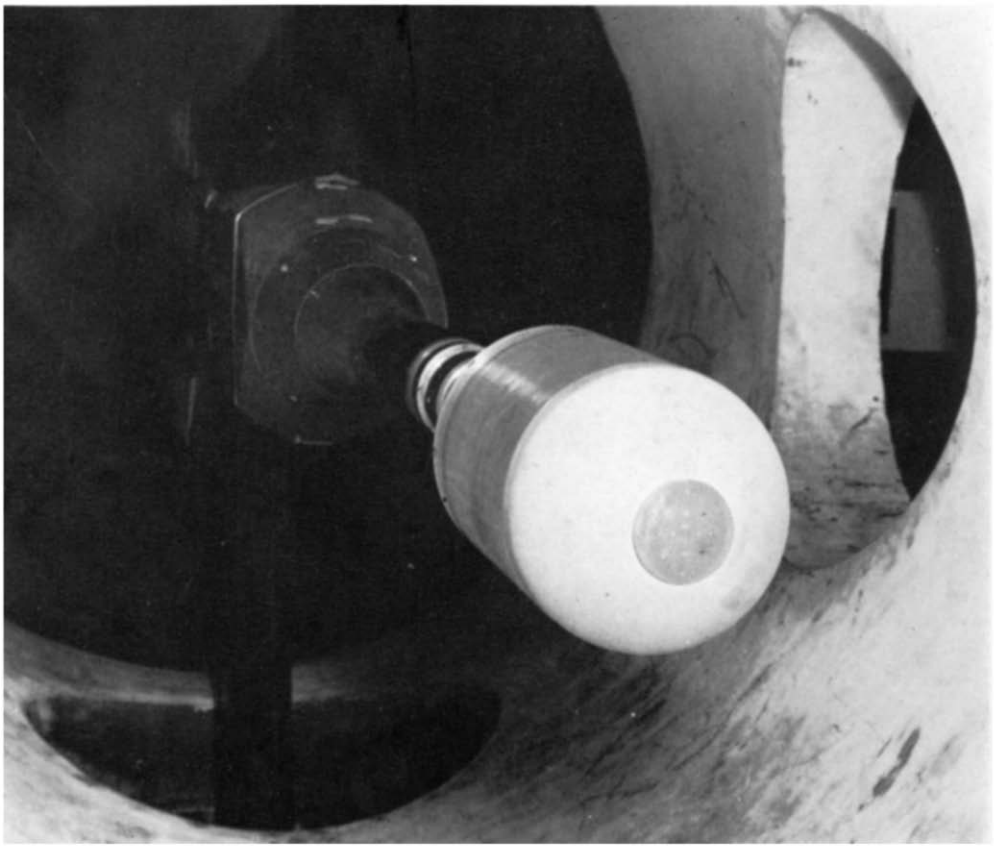

FIG. 2. Model mounted in tunnel "B", VKF, AEDC.

[*facing p.* 702]

ice–silicone bath was included in the supply system. The bath temperature was approximately −100°F which was very close to the freon-13 liquefaction temperature. Since condensation could not be tolerated, the bath had to be bypassed. In view of the low thermal capacity of freon-13, this severely limited the possible T_w range. In the case of helium, the bath was most effective.

Primary coolant temperature control was achieved by means of an electric heater mounted within the model. This heater consisted of a cylinder of porous inconel, 8 in long by $1\frac{3}{4}$ in dia., in which was embedded a coil of sheathed nichrome wire. The heater temperature was monitored by means of the thermocouple shown in Fig. 1. Two variable output transformers in series furnished precise heater temperature control. Maximum heater output was about 2·5 kW, corresponding to a T_h of 1220°F and a helium mass flow of 0·00182 lb/s.

2.4 *Test facility*

The test was carried out in wind tunnel "B" of the von Kármán Gas Dynamics Facility (VKF) at the Arnold Engineering and Development Center [14], Arnold Air Force Station, Tenn.* This is a continuous flow, closed circuit tunnel, having a fixed Mach number, axisymmetric nozzle and a 50 in diameter test section. Both nozzle and test section walls are water cooled, as is most of the sting and sector on which the model was mounted. The nominal test section Mach number is 8·0, at a constant stagnation temperature of 900°F. Tunnel stagnation pressure may be varied between 100 and 800 psia. All pressure and temperature data was automatically recorded and reduced by an ERA-1102 digital computer [14].

2.5 *Test procedure*

The model was mounted in tunnel "B" with its nose 2·5 in upstream of the centerline of the test section windows. Initial runs were devoted to checking zero angle of attack and obtaining no-injection surface temperature distributions. The non-dimensionalized blowing parameter appropriate to the test geometry is given by [2]

$$f_w = -(\rho v)_w (2\rho\mu)_e^{-1/2} \left(\frac{du}{dx}\right)_e^{-1/2} \tag{4}$$

in which the fluid properties are evaluated at the outer edge of the boundary layer, and the velocity gradient is computed by assuming a Newtonian pressure distribution on the hemisphere. The definition of f_w is seen to be independent of injectant properties. The injection levels tested were −0·2, −0·4, −0·6, −0·8, and −1·0 for helium, and −0·2, −0·6, −0·8, and −1·0 for freon-13. For test purposes the injection distribution over the porous cap was assumed to be uniform, so that for each injection level the corresponding total coolant flow was simply $(\rho v)_w$ times the cap area. This flow was then set and held constant as described in Section 2.3.

Due to the radiation losses to the cold test section walls, it was not possible to compute T_c settings prior to the test. For most injection levels, four levels of $\bar{T}_w$ were obtained. Normally the lowest practicable level was obtained first. For helium the lower limit was $\bar{T}_w = 0{\cdot}5$; for freon-13, about 0·8. The highest was specified as near 1·2 for helium and 1·0 for freon-13 and the remaining levels spaced at equal intervals between these limits.

No attempt was made to vary $\bar{T}_w$ once the initial setting of $\bar{T}_c$ was made. This procedure minimized the time taken to achieve thermal equilibrium. In practice, $\bar{T}_c$ and $\bar{T}_h$ were monitored continuously together with key surface thermocouples on the model surface. When these readings were constant, a check was made of all thermocouple and pressure readings before the data was finally recorded. Average overall time for a run was 40 min.

3. RESULTS

3.1 *Tunnel conditions*

Average stagnation temperature during the test was 1346°R, and average free stream Reynolds number was $3{\cdot}38 \times 10^6$/ft. On the basis of tunnel calibration data, the Mach number at the bow-shock location was taken to be 8·07. The boundary layer was laminar. Static pressure

* The author wishes to thank O. R. Pritts and other VKF personnel for their help during the wind tunnel test.

measurements taken on the model indicate the yaw angle was less than 1°.

3.2 *Injection distribution*

The flow per unit area through the porous cap is approximated by the following expression [15]:

$$p_c^2 - p_e^2 = 2(\mu RT)_w (\rho v)_w \alpha t \qquad (5)$$

It is assumed that the flow rate is small and the wall isothermal. The porous material properties appear in the viscous resistance coefficient (α) and the thickness (t), both of which are constant. The gas characteristics appear in the viscosity and in the gas constant (R). If equation (5) is solved for $(\rho v)_w$ and the result normalized with respect to stagnation point ($\theta = 0$) values αt cancels out. Integration of the result over the surface gives an effective area which includes the effects of non-uniform pressure drop and surface temperature. When this is divided into the total coolant flow, as measured by the orifice, the stagnation point injection rate is obtained. It should be noted that this technique largely eliminates errors due to the plug not being locally isothermal. Temperature differences across the plug of up to 40 degF were observed with helium injection. However, errors introduced by using T_w instead of some average temperature in equation (5) will be cancelled out by the normalization.

From equation (5) it can be seen that, due to the higher molecular weight (i.e. lower R), the pressure drop required to pass a given flow of freon-13 is much less than for helium. The maximum design p_c was 20 psia, corresponding to the highest helium flow at maximum T_w. As a result, for freon-13 the difference between p_c and p_e was of the same order of magnitude as the anticipated measuring accuracy. Thus no precise computation of the injection distribution was possible. Instead an average blowing rate, based on the total coolant flow and cap area, was obtained. For zero injection, T_{aw} over the cap ($0 < \theta < 20°$) should be constant to within $\frac{1}{2}$ per cent; similarly, the maximum decrease in h is less than 8 per cent. Assuming the same magnitudes to hold with injection, the above averaging process should introduce little error, except for that arising from the non-uniform injection distribution. The method used for helium, of course, yields a true stagnation point injection rate.

3.3 *Surface temperature distributions*

Typical surface temperature distributions, uncorrected for radiation effects, appear in Fig. 3. Temperatures on the porous cap were not uniform, particularly with freon-13 injection.

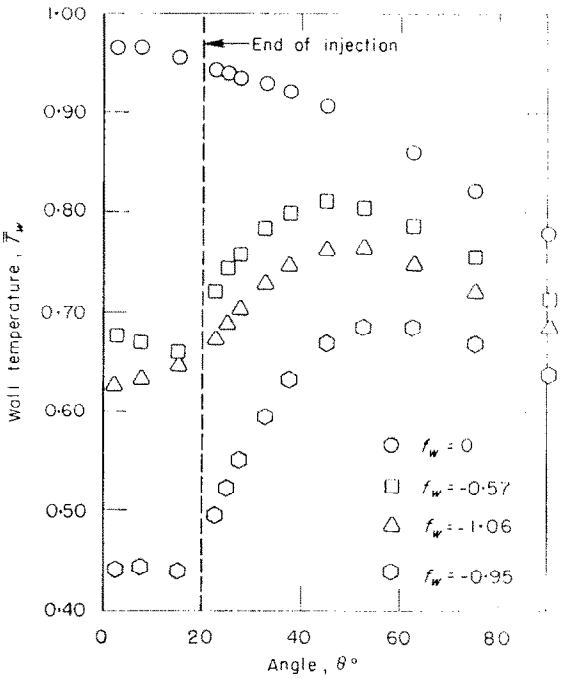

FIG. 3(a). Surface temperature distributions with helium injection.

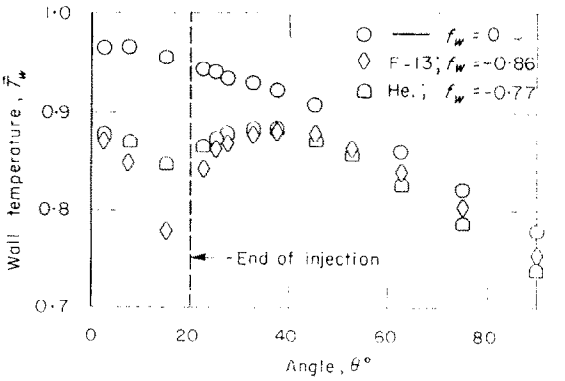

FIG. 3(b). Surface temperature distributions with helium and freon-13 injection.

In keeping with the injection rate computing procedures discussed in the preceding section, a stagnation point wall temperature was obtained by extrapolation for the helium runs, while for freon-13 an average value was obtained by integration over the cap area. These values were used in the computations discussed in succeeding sections.

In Fig. 3(a) temperature distributions for various helium injection rates and cap temperatures are compared. It is clear that upstream injection lowers the recovery temperature over the entire insulated region. The downstream temperature level is strongly effected by the initial temperature on the cap. The occurrence of a temperature peak near 50° was observed also in reference 12, and probably arises from the fact that the heat flux level decreases rapidly downstream on the hemisphere, and tends to more than offset the decay in effectiveness of the upstream injection. It appears that increased injection and/or lowered cap temperatures tend to move this peak farther aft on the hemisphere.

It might be concluded from Fig. 3(a) that a large increase in injection level has but small effect downstream of the porous cap. However, this is not necessarily true for all injection levels. Though the total mass fluxes differ by a factor of two, from the standpoint of injection concentration at the wall (c_{1w}) there is little difference between an f_w of $-0{\cdot}57$ and $-1{\cdot}06$; the theoretical concentration [9] being 95 per cent for the former rate and $\sim$100 per cent for the latter. In other words, an almost pure layer of helium exists (at least initially) on the surface in both cases. Farther downstream, of course, a higher total injection rate should result in slower decay of the insulating effect; this seems to be true from Fig. 3(a). On this basis, an increase in f_w from say $-0{\cdot}2$ to $-0{\cdot}4$ might be expected to have relatively larger downstream effect. Unfortunately, suitable data for such a comparison is lacking.

A comparison of the downstream influence of helium and freon-13 injection appears in Fig. 3(b). Unfortunately neither the injection rates nor the porous wall temperatures are the same; however, it is apparent that for freon-13 the downstream recovery temperature does increase more rapidly. This should be expected, in view of freon-13's lower heat capacity. Undoubtedly, at lower cap temperatures the disparity between the two coolants would be larger.

3.4 *Internal temperature distribution*

Contrary to expectations, the two plenum thermocouples (Section 2.1) did not give identical values for T_c. In general, both readings were less than the heater temperature (T_h). However, the thermocouple nearer the porous cap always read higher than the other, indicating that the coolant was absorbing heat from the plenum walls via the glass wool as it flowed toward the cap. This situation was independent of the cap temperature, i.e. whether the coolant was hot or cold relative to the cap. One must conclude, therefore, that the true value of T_c appropriate for use in equation (3) lay between the plenum reading closer to the cap, and the temperature on the inner surface of the cap itself. Since no better value was available, the former reading was used throughout to compute $\dot{q}$.

This source of uncertainty did not prove to be a serious one. The potential uncertainty introduced in the heat flux (and hence in the T_{aw}) computations was greater for helium, since it was magnified by the large specific heat of that gas. For either gas, the error would be small for the low heat-transfer case ($T_w \approx T_{aw}$) for which the temperature gradients were everywhere small. For the high heat-transfer runs ($T_w - T_c$) was large (particularly for freon-13) and so, percentagewise, the error would still be small. It should be noted that the use of this approach must lead to high values of $\dot{q}$, since by the above argument, the resulting coolant temperature rise ($T_w - T_c$) will be greater than or equal to the true value. For helium injection, T_c ranged from 570° to 1500°R; for freon-13, from 870° to 1330°R.

3.5 *Adiabatic wall temperatures*

The adiabatic wall temperature for each coolant injection rate was obtained from a plot of heat flux versus T_w of which Fig. 4 is an example. The injection rate, wall and coolant temperatures were obtained as described in preceding sections, and substituted in equation (3). A radiation correction was added to obtain the total heat flux absorbed by the injectant.

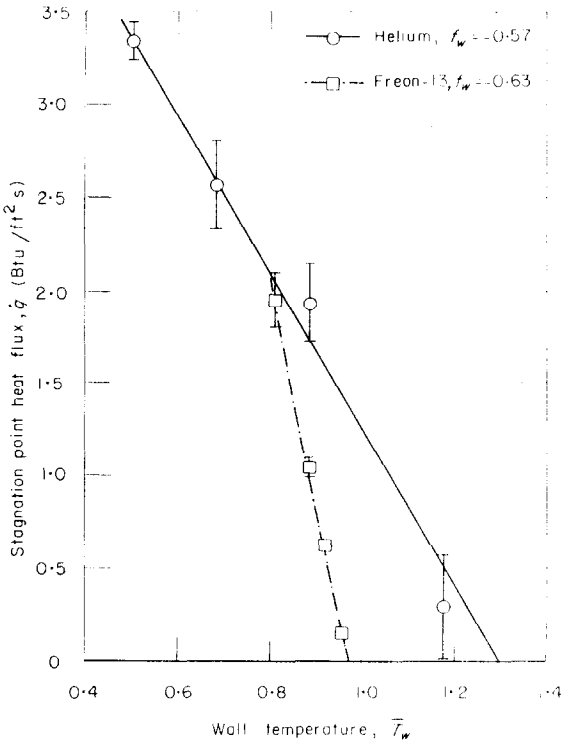

FIG. 4. Variation of heat flux with wall temperature; for helium and freon-13 injection.

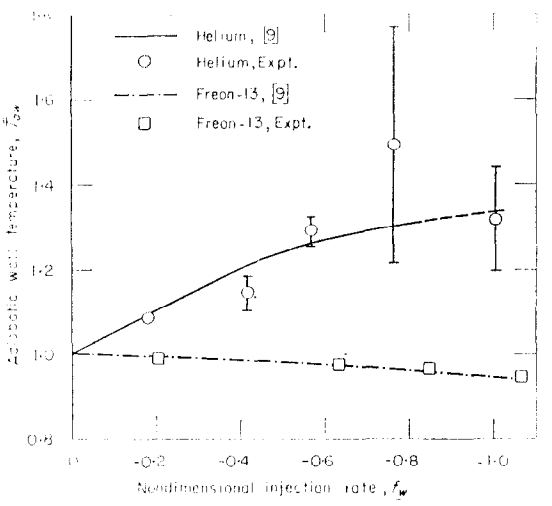

FIG. 5. Adiabatic wall temperature versus injection rate for helium and freon-13.

Since the hot nozzle throat constituted a negligible part of the total field of view for the model, the nozzle could be treated as a black body having a uniform temperature of 70°F. The effective emissivity was obtained from comparison of the measured no injection temperature distribution (Fig. 3) with the theoretical recovery temperature distribution and the heat loss due to radiation computed as a function of the stagnation point surface temperature.

The lines in Fig. 4 represent constant slope fits to the data. $\bar{T}_{aw}$ is given by the intersection of each line with the $\bar{T}_w$-axis. The uncertainty bands shown in Fig. 4 are largely due to the basic sensitivity of the thermocouples (Section 2.1). Since this uncertainty is multiplied by the specific heat [equation (3)], the band width is proportionately larger for helium than for freon-13 (for which it is of the same order as the symbols used).

The variation of adiabatic wall temperature with injection rate appears in Fig. 5, for both coolants. Agreement with the stagnation point values of reference 9 is satisfactory. It is inferred from the self-consistency of the freon-13 data that no serious error was introduced by the averaging technique described in previous sections. It would appear that the data confirms the dependence of the adiabatic temperature on both the magnitude and sign of the thermal diffusion ratio (k_T).

3.6 *Heat-transfer coefficient*

The heat-transfer coefficient, expressed in terms of a zero injection, stagnation point value, was computed from the following expression.

$$\overline{St} = \frac{\dot{q}}{[St\sqrt{(Re)}]^* \, c_{pe} \, (T_{aw} - T_w) \, (2 \, \rho\mu)_e^{1/2} \left(\frac{du}{dx}\right)_e^{1/2}} \tag{6}$$

$[St\sqrt{(Re)}]^*$ was obtained from reference 9, and is the zero injection value for the appropriate $\bar{T}_w$.

The results appear in Fig. 6(a) and (b) for helium and freon-13 respectively. For helium the temperature difference $(\bar{T}_{aw} - \bar{T}_w)$ was almost always large, so that there was little increase in scatter as compared with the heat

flux. On the other hand the freon-13 runs, as has already been mentioned, were all relatively "warm" and this fact, coupled with the lower $\bar{T}_{aw}$ level, resulted in increased uncertainty arising from instrumentation accuracy.

The results from reference 9 normalized with respect to $[St\sqrt{(Re)}]^*$ also appear in Fig. 6. The resulting $\overline{St}$ is almost independent of $\bar{T}_w$ over the experimental range. Similarly, theory predicts that thermal diffusion will have little effect on $\overline{St}$; thus only the curve for $k_T \neq 0$ is presented. The computations of Hoshizaki and Smith [3] give a curve virtually identical to reference 9.

Agreement between theory and experiment is satisfactory. The fact that the heat-transfer data is mostly higher than theory may be due to the somewhat arbitrary definition of $\bar{T}_c$ (Section 3.4). It is possible that the non-uniform freon-13 injection distribution may also have been a contributing factor.

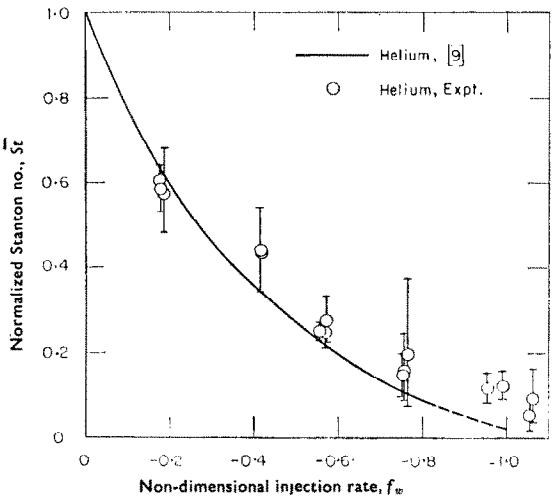

FIG. 6(a). Non-dimensional heat-transfer coefficient versus helium injection rate.

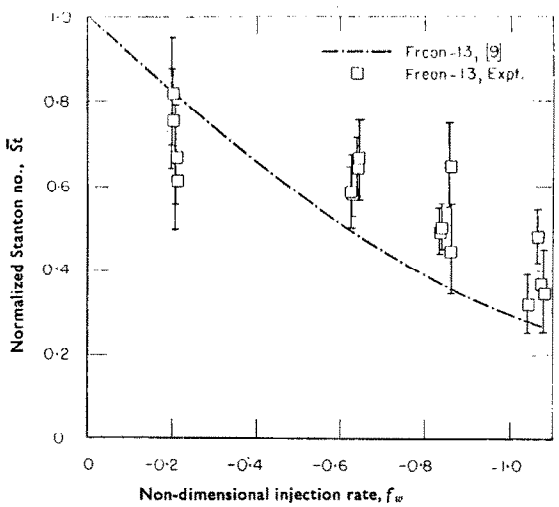

FIG. 6(b). Non-dimensional heat-transfer coefficient versus freon-13 injection rate.

4. CONCLUSION

The results of the experimental study are in reasonable agreement with theoretical computations carried out for mass transfer at an axisymmetric stagnation point. For both freon-13 and for helium, the anticipated reduction in Stanton number with increasing injection rate is apparent. In addition, the marked dependence of adiabatic wall temperature on both the coolant and the blowing rate is substantiated. The only modification to the earlier analyses (which did not predict this dependence) was the inclusion of thermodynamic coupling in the appropriate boundary-layer equations. It seems reasonable therefore, to attribute the present consistency between theory and experiment to this particular source.

Observed adiabatic temperature distributions on the hemispherical surface, downstream of the injection region, indicate that substantial cooling may be achieved over the entire nose by localized injection. Helium appears to be more effective in this respect.

REFERENCES

1. J. R. BARON, The binary-mixture boundary layer with mass transfer cooling at high speeds, MIT, Naval Supersonic Laboratory, *TR* 160, May (1956).
2. J. R. BARON and P. B. SCOTT, The laminar diffusion boundary layer with external flow field pressure gradients, MIT, Naval Supersonic Laboratory *TR* 419, December (1959).
3. H. HOSHIZAKI and H. J. SMITH, Axisymmetric stagnation point mass transfer cooling, Lockheed Missiles and Space Division, *TR LMSD*-48381, January (1959).
4. G. E. ANDERSON, C. J. SCOTT and D. R. ELGIN, Mass transfer experiments on a hemisphere at $M = 5$, University of Minnesota, Rosemount Aero Labs, *RR* 166, August (1959).
5. A. F. GOLLNICK Jr., Thermal effects on a transpiration-cooled hemisphere, *J. Aero. Space Sci.* **29**, 583–591 (1962).

6. O. E. TEWFIK, E. R. G. ECKERT and L. S. JUREWICZ, Diffusion thermo effects on heat transfer from a cylinder in cross flow, *J. Amer. Inst. Aero. Astro.* **1**, 1537–1543 (1963).
7. O. E. TEWFIK, E. R. G. ECKERT and C. J. SHIRTLIFFE, Thermal diffusion effects on energy transfer in a turbulent boundary layer with helium injection. *Proceedings*, 1962 *Heat Transfer and Fluid Mechanics Institute*, Stanford University Press, Stanford, Cal. 42–61 (1962).
8. J. R. BARON, Thermodynamic coupling in boundary layers, *J. Amer. Rocket Soc.* **32**, 1052–1059 (1962).
9. J. R. BARON, Thermal diffusion effects in mass transfer, *Int. J. Heat Mass Transfer* **6**, 1023–1033 (1963).
10. F. E. C. CULICK, An integral method for calculating heat and mass transfer in laminar boundary layers, *J. Amer. Inst. Aero. Astro.* **1**, 1097–1104 (1963).
11. A. F. GOLLNICK Jr. Insulating properties of a boundary layer downstream of a transpiration cooled region. IAS Fairchild Fund Paper *FF*-30, 41–44, January (1962).
12. P. A. LIBBY and R. J. CRESCI, Experimental investigation of the downstream influence of stagnation-point mass transfer, *J. Aero. Space Sci.* **28**, 51–64 (1961).
13. Du Pont de Nemours & Co., Inc., Thermodynamic Properties of Freon-13, Technical Bulletin *T*-13 (1959).
14. *Arnold Center Test Facilities Handbook*, Vol. 4, pp. 3.1–3.5, 5.1–5.4. Arnold Air Force Station, Tennessee, January (1961).
15. L. GREEN Jr. and P. DUWEZ, Fluid flow through porous metals, *J. Appl. Mech.* **18**, 39–45 (1951).

Résumé—Un modèle hémisphérique ayant au nez une calotte poreuse de 40° d'angle total a été essayé au nombre de Mach 8,07. De l'hélium et du fréon-13 étaient injectés à travers la calotte dans la région d'arrêt, et on a mesuré les variations de la température adiabatique de paroi et du coefficient de transport de chaleur avec le débit d'injection. On a obtenu des solutions analytiques pour une couche limite laminaire au point d'arrêt et des conditions semblables dans l'écoulement libre. L'analyse diffère d'un travail précédent en ce que les effets de la diffusion thermique sont inclus. On prédit que ce couplage thermodynamique peut conduire à des températures de frottement au point d'arrêt considérablement différentes de la valeur pour une injection nulle. Cette conclusion, et donc le sens du couplage thermodynamique, est appuyée par les données, qui sont en accord raisonnable avec la theorie. Les mesures de températures étaient faites sur la surface isolée du modèle en aval de la région d'injection. On a conclu que les niveaux de températures sur toute surface hémisphérique peuvent être réduits grandement par une injection localisée dans la région d'arrêt. L'hélium s'est démontré être plus efficace en ceci que le fréon-13.

Zusammenfassung—Ein halbkugelförmiges Modell mit einer porösen Kappe von einer Grösse, die dem Öffnungswinkel 40° entsprach, wurde bei Mach 8,07 untersucht. Helium und Frigen 13 wurden durch die Kappe in den Staubereich eingespritzt und die Änderung der adiabaten Wandtemperatur und des Wärmeübergangskoeffizienten mit der Einspritzmenge gemessen. Analytische Lösungen liessen sich für laminare Grenzschicht am Staupunkt und ähnliche Freistrombedingungen erhalten. Die Analysis unterscheidet sich von anderen Arbeiten darin, dass die Einflüsse der Thermodiffusion berücksichtigt sind. Diese thermodynamische Kopplung könnte am Staupunkt auf Rückgewinntemperaturen führen, die wesentlich vom Wert für Einspritzung Null abweichen. Diese Annahme und damit die Bedeutung der thermodynamischen Kopplung wird von den Daten gestützt, die mit der Theorie verhältnismässig gut übereinstimmen. Temperaturmessungen erfolgten an der isolierten Modelloberfläche stromabwärts vom Einspitzbereich. Vermutlich können die Temperaturen an der gesamten Halbkugelfläche durch örtlich begrenzte Einspritzung in den Staupunktsbereich weitgehend gesenkt werden. Helium ist dabei wirkungsvoller als Frigen 13.

Аннотация—Исследовалась полусферическая модель, имеющая пористую насадку под углом 40° при $M = 8{,}07$. Гелий и фреон-13 вдувались через насадок в критическую область; измерялись изменения адиабатической температуры стенки и коэффициента теплообмена в зависимости от скорости вдува. Получены аналитические решения для ламинарного пограничного слоя в критической точке и для подобных условий свободного потока. Этот анализ отличается от ранее проделанной работы тем, что он учитывает эффекты термодиффузии. Найдено, что это термодинамическое взаимодействие может привести к температурам восстановления в критической точке, которые значительно отличаются от нулевого значения вдува. Этот вывод, а, следовательно, и термодинамическое взаимодействие подтверждается данными, хорошо согласующимися с теорией. Измерялась температура на изолированной поверхности, находящейся вниз по потоку в области вдува. Можно сделать вывод, что температурные уровни на всей полусферической поверхности могут быть сильно уменьшены путем локального вдува в критическую область. Оказалось, что гелий более эффективен, чем фреон-13 в этом отношении.